MINISTRY OF EDUCATION AND TRAINING

VIETNAM ACADEMY OF SCIENCE AND TECHNOLOGY

GRADUATE UNIVERSITY OF SCIENCE AND TECHNOLOGY

ĐINH THỊ TÚ

ISOLATION, PURIFICATION OF CURCUMIN AND SEMI-SYNTHESIS OF ITS DERIVATIVES GUIDED BY *in vitro* AND *in silico* BIOLOGICAL ACTIVITIES FROM VIETNAMESE TURMERIC (*Curcuma longa* L.)

SUMMARY OF DISSERTATION ON SCIENCES OF MATTER

Major: Natural Products Chemistry

Code: 9 44 01 17

HA NOI – 2026

The dissertation is completed at: Graduate University of Science and Technology, Vietnam Academy of Science and Technology

Supervisors:

1. Supervisor 1: Associate Professor, Dr. Pham Minh Quan
   Institute of Chemistry - Vietnam Academy of Science and Technology
2. Supervisor 2: Associate Professor, Dr. Ngo Kim Chi
   Institute of Chemistry - Vietnam Academy of Science and Technology

Reviewer 1: Associate Professor, Dr. Nguyen Thi Hong Van, Institute of Chemistry - Vietnam Academy of Science and Technology

Reviewer 2: Associate Professor, Dr. Pham Thi Tam, Hanoi Open University

The dissertation is examined by Examination Board of Graduate University of Science and Technology, Vietnam Academy of Science and Technology at 2:30 p.m. on 2 July 2026.

The dissertation can be found at:

1. Graduate University of Science and Technology Library
2. National Library of Vietnam

LIST OF THE PUBLICATIONS RELATED TO THE DISSERTATION

1. **Tu Thi Dinh**, Quan Minh Pham, Long Quoc Pham, Chi Kim Ngo, Van Thi Thuy Nguyen, Thuong Thi Le Hoang, Tu Ngoc Ly, Linh Ngoc Nguyen, Thao Thi Phuong Nguyen and Lam Tien Do, 2026, Impact of *Scutellonema curcumae* sp. n. (Nematoda: Hoplolaimidae) on the Phytochemical Profile and Biological Activities of Turmeric (*Curcuma longa* L.), *Molecules*, 31(6), 920.

2. **Dinh Thi Tu**, Ngo Kim Chi, Le Thi Thuy Huong, Do Huu Nghi, Pham Minh Quan, 2026, *In silico* and *in vitro* investigation of curcuminoid as potential TLR4/MD-2 complex inhibitors using molecular docking and molecular dynamic simulations, *Vietnam Journal of Science and Technology*, https://doi.org/10.15625/2525-2518/24045.

3. Dinh Hieu Truong, **Thi Tu Dinh,** Thi My Duyen Trinh, Thi Hong Minh Pham, Minh Quan Pham, Urszula Gawlik-Dziki and Duy Quang Dao, 2025, HOO radical scavenging activity of curcumin I and III in physiological conditions: a theoretical investigation on the influence of acid-base equilibrium and tautomerism, *RSC Advances*, 15(8), 5649-5664.

4. Phi Hung Nguyen, Anh Tuan Nguyen, **Thi Tu Dinh**, Dao Cuong To, Thi Phuong Hoang, Ngoc Quang Dang, Thi Thuy Do, Thi Ha Vu, Thi Thuc Bui, Thi Thu Ha Trinh, 2023, Methodology for quick analysis of curcumin, demethoxycurcumin and bisdemethoxycurcumin from turmeric by Agilent 1260 HPLC system, *The University of Danang - Journal of Science and Technology,* 21*(*5), 103-109.

INTRODUCTION

Rationale

Turmeric (*Curcuma longa* L., Zingiberaceae) is an important medicinal plant in Vietnamese traditional medicine, valued for its anti-inflammatory, antibacterial, antioxidant, hepatoprotective and digestive properties. Its rhizomes contain a curcuminoid complex of three structurally related compounds: curcumin (CUR), demethoxycurcumin (DMC) and bisdemethoxycurcumin (BDMC) with a broad spectrum of biological activities.

Although the most extensively studied curcuminoid, CUR has not become a clinical drug because of its low oral bioavailability. Two structural weaknesses underlie this: the central β-diketone system is readily reduced by phase-I enzymes, and the phenolic hydroxyl groups undergo glucuronidation and sulfation in phase II. These liabilities motivate semi-synthetic modification. The individual curcuminoids have also not been compared within a single assay panel; and in Vietnam, neither the nematode species parasitizing turmeric rhizomes nor the relationship between infestation level and individual curcuminoid content has been systematically investigated.

This dissertation therefore adopts a multidisciplinary approach integrating synthetic chemistry, experimental pharmacology, *in silico* modeling (molecular docking, molecular dynamics and DFT calculations) and nematode biology to evaluate the medicinal value of Vietnamese turmeric. It is entitled: "Isolation, purification of curcumin and semi-synthesis of its derivatives guided by *in vitro* and *in silico* biological activities from Vietnamese turmeric (*Curcuma longa* L.)".

Research objectives

This dissertation aims to enhance the biological value of the curcuminoid system from Vietnamese turmeric (*C. longa*) by isolating its pure constituents, assessing the impact of an ecological factor (parasitic nematodes) on raw-material quality, and semi-synthesizing novel

derivatives. *In vitro* bioassays and *in silico* tools are combined to evaluate these activities and elucidate their mechanisms at the molecular level, providing a scientific basis for developing new medicinal preparations.

Research contents

The dissertation addresses the following four research objectives:

1. To establish a procedure for the isolation and separate extraction of the individual curcuminoids (CUR, DMC and BDMC) from Vietnamese turmeric rhizomes.

2. To evaluate the correlation between nematode density and the content and biological activities of the curcuminoids.

3. To semi-synthesize and structurally characterize novel derivatives: the curcumin-zerumbone hybrids (curcumin-monozerumbone and curcumin-biszerumbone) and di-propargyl curcumin and to investigate their biological activities.

4. To screen and elucidate the mechanisms underlying the principal biological activities of the three purified curcuminoids by *in silico* simulation combined with *in vitro* assays, including antioxidant activity (DPPH assay).

Novel contributions of the dissertation

- The nematode *Scutellonema curcumae*, parasitizing turmeric rhizomes in Vietnam, was discovered and identified for the first time. Increasing nematode infestation density was shown to reduce the curcuminoid content of the medicinal material: the least-infested group showed markedly higher antioxidant activity than the most heavily infested, its SC_{50} value falling from 43.62 to 13.85 μg/ml.

- The novel hybrid derivative curcumin-monozerumbone (4) was successfully semi-synthesized, improving lipophilicity (logP increasing from 3.72 to 6.51) relative to natural curcumin. This molecular design proved optimal with respect to biological activity: it exhibited greater anti-inflammatory potency and stronger cytotoxicity towards hepatocellular carcinoma (Hep-G2) cells than the curcumin control, while broadening the

antimicrobial spectrum (6/8 test strains inhibited, against only 2/8 for curcumin).

- An interdisciplinary *in silico* approach (DFT quantum calculations, molecular docking and molecular dynamics simulation) was applied for the first time to elucidate the structure–activity basis of the curcuminoid system. The calculations confirmed that BDMC possesses an appreciably higher rate constant for HOO• radical scavenging in the lipid environment than CUR, proceeding predominantly by hydrogen-atom transfer. MD simulation further demonstrated that BDMC forms a more stable complex with the TLR4/MD-2 target protein (binding energy -9.73 kcal/mol versus -9.29 kcal/mol for CUR), thereby accounting for the inhibition of nitric oxide (NO) observed experimentally.

Dissertation structure

The dissertation comprises 125 pages, organized into 3 main chapters (in addition to the Introduction and Conclusions), with 19 tables, 27 figures and 147 references.

CHAPTER 1. LITERATURE REVIEW

This chapter synthesizes the foundational knowledge on *C. longa*, including botanical characteristics, ecological distribution, chemical composition, and biological activities of curcuminoids.

1.1. Overview of the genus *Curcuma* L.

The genus *Curcuma* belongs to the Zingiberaceae family, comprising approximately 70-80 species of perennial rhizomatous herbs. Its chemical composition comprises diverse classes of compounds, including phenolics, flavonoids, alkaloids, terpenoids, tannins and saponins. To date, nearly 720 compounds have been identified, with sesquiterpenoids and diarylheptanoids as the principal constituents.

1.2. Overview of turmeric (*Curcuma longa* L.)

Turmeric originates from India and is now widely cultivated in tropical countries, with Vietnam being an important source region. *C. longa* is a perennial herbaceous species attaining a height of approximately 60 cm. The rhizome is brown externally, with an orange to bright yellow inner flesh, a pungent aroma and an acrid, bitter taste.

1.3. Structure and physicochemical properties of the curcuminoid system

The curcuminoid system accounts for approximately 2-8% of dried turmeric rhizome mass, comprising three principal components that always coexist. All three derivatives belong to the diarylheptanoid class with a basic scaffold consisting of two aromatic rings connected by a 7-carbon chain. The key structural difference lies in the methoxy ($-OCH_3$) substituents on the aromatic rings: CUR with 2 methoxy groups (70-80%); DMC with 1 methoxy group (15-20%); BDMC with no methoxy groups (2-5%). Under harsh conditions (alkaline, thermal, oxidative), the stability order is established as BDMC > DMC > CUR. The absence of methoxy substituents renders BDMC less susceptible to UV-Vis irradiation than the other two derivatives.

1.4. Biological activities and specific molecular mechanisms

Current research is increasingly focused on BDMC due to its valuable pharmacological mechanisms: BDMC demonstrates superior inhibition of iNOS enzyme compared to curcumin; BDMC acts as a GPR161 receptor inhibitor, blocking the mTOR signaling pathway and promoting apoptosis in cancer cells (particularly triple-negative breast cancer). Due to lower degradation rates, BDMC maintains therapeutic concentrations in tissues longer than CUR, overcoming the rapid elimination disadvantage of the principal derivative.

1.5. *In silico* research methods

The dissertation applies modern computational tools for atomic-level mechanism elucidation: quantum chemical calculations (DFT) using Gaussian 16 with the M06-2X functional to investigate antioxidant

mechanisms through thermodynamic parameters (BDE, IP, PA); molecular simulations (Docking & MD) using AutoDock and GROMACS to evaluate interactions between curcuminoids and protein targets TLR4/MD-2.

1.6. Parasitic nematodes and their impact on medicinal plant quality

Root nematodes (particularly the genera *Scutellonema* and *Meloidogyne*) are hazardous pests that not only reduce yields but also cause biological stress, disrupting curcuminoid accumulation.

CHAPTER 2. MATERIALS AND METHODS

2.1. Curcuminoid derivative synthesis

2.1.1. Curcumin-zerumbone derivatives

Semi-synthesis was performed in two stages: (i) Bromination of zerumbone with NBS in CH_3CN:H_2O (1:1), yielding 3-bromozerumbone (> 95% yield); (ii) Nucleophilic substitution of curcumin with 3-bromozerumbone using K_2CO_3 base in DMF, at room temperature, for 12 h. Purification by column chromatography and semi-preparative HPLC afforded curcumin-monozerumbone (15% yield) and curcumin-biszerumbone (11% yield). Structures were determined by ^{1}H-NMR, ^{13}C-NMR, and HR-MS.

2.1.2. Di-propargyl curcumin derivative

Synthesis was performed via the Williamson ether synthesis: curcumin was reacted with propargyl bromide (2.5 equiv.) and K_2CO_3 (3.0 equiv.) in anhydrous DMF at room temperature for 24 h. *O,O′*-di-propargyl curcumin ($C_{27}H_{24}O_6$, 21% yield) was characterized by NMR and HR-MS.

2.2. *In vitro* biological activity evaluation

Four assay groups were conducted: (i) Antioxidant activity by the DPPH method (λ = 517 nm, positive control: ascorbic acid); (ii) Anti-inflammatory activity via NO inhibition on RAW 264.7 cells stimulated with LPS (Griess reagent, λ = 540 nm); (iii) Cytotoxicity against 5 human cancer

cell lines (Hep-G2, HeLa, MCF-7, A549, HGC-27) by the MTT assay (positive control: Paclitaxel); (iv) Antimicrobial activity by broth microdilution MIC determination on 4 bacterial and 4 fungal strains.

2.3. *In silico* studies

HOO• radical scavenging activity was predicted by DFT (M06-2X/6-311++G(3df,3pd)) in aqueous and lipid (PEA) environments, examining three mechanisms: HAT (Abs), RAF (Add), and SET. Anti-inflammatory mechanisms were elucidated by molecular docking (AutoDock 4.2.6, LGA) and molecular dynamics simulations (GROMACS, Amber99SB-iLDN/GAFF) with the TLR4/MD-2 complex (PDB: 2Z64, 3VQ2). ADMET profiles were evaluated using Molinspiration, ProTox-II, and admetSAR.

2.4. Nematode research

Nematodes were isolated using the modified Baermann tray method. Identification was based on morphology (Olympus BX51 microscope) combined with molecular biology (sequencing of D2-D3/28S rDNA, ITS, and COI mtDNA regions; phylogenetic analysis using MrBayes). The impact of nematode infestation on curcuminoid content was quantified by HPLC (Agilent 1260, Eclipse XDB-C18 column, $\lambda = 428$ nm).

CHAPTER 3. RESULTS AND DISCUSSION

3.1. Isolation and structural characterization

Three principal curcuminoid compounds were successfully isolated from Vietnamese turmeric rhizomes (*C. longa* L.): CUR, DMC, BDMC. These compounds were isolated with high purity through modern chromatographic methods and structurally characterized by ^{1}H-NMR and ^{13}C-NMR spectroscopy, with data consistent with literature reports.

3.1.1. Curcumin (CUR)

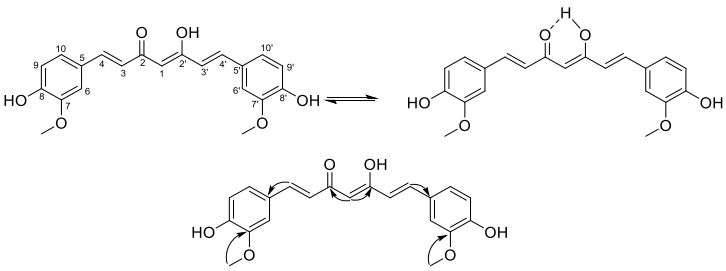

Figure 3.1. Chemical structure of the CUR compound

Table 3.1. ^{1}H and ^{13}C-NMR spectral data for compound CUR

No	CUR		[144]	
	$^{a}\delta_C$ ppm	**$^{a}\delta_H$ ppm (*J*; Hz)**	**#δ_C ppm**	**#δ_H ppm (*J*; Hz)**
1	101.1	5.80 (s)	100.9	5.98 (s)
2, 2′	183.3	-	183.4	16.41 (s)
3, 3′	121.8	6.49 (d; 15.6)	121.1	6.73 (d; 16.0)
4, 4′	140.6	7.60 (d; 15.6)	140.7	7.53 (d; 16.0)
5, 5′	127.7	-	126.4	-
6, 6′	109.7	7.04 (s)	111.4	7.32 (d; 2.0)
7, 7′	146.8	-	148.0	-
8, 8′	147.9	-	149.4	9.74 (s)
9, 9′	114.9	6.94 (d; 8.4)	115.7	6.85 (d; 8.1)
10, 10′	122.9	7.12 (d; 6.6)	123.2	7.16 (dd; 2.0; 8.1)
OCH_3	56.0	3.94 (s)	55.7	3.84 (s)
-OH	-	5.89 (1H, br s)		

[a]$CDCl_3$ at 600 MHz (^{1}H-NMR) and 150 MHz (^{13}C-NMR)

[#] DMSO-d_6 at 500 MHz (^{1}H-NMR) and 125 MHz (^{13}C-NMR)

3.1.2. Demethoxycurcumin (DMC)

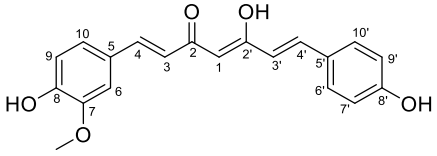

Figure 3.2. Chemical structure of the DMC

Table 3.2. ^{1}H and ^{13}C-NMR spectral data for compound DMC

No	DMC		[145]	
	$^{a}\delta_C$ ppm	**$^{a}\delta_H$ ppm (*J*; Hz)**	**#δ_C ppm**	**#δ_H ppm (*J*; Hz)**
1	100.9	5.82 (s)	102.0	5.98 (s)
2	183.3	-	184.8	-
3	121.1	6.53 (dd; 15.5; 3.0)	122.3	6.64 (d; 15.8)
4	140.7	7.63 (d; 15.5)	142.1	7.59 (d; 15.8)
5	126.4	-	128.6	-
6	111.2	7.09 (d; 2.0)	111.7	7.23 (d; 1.9)
7	148.0	-	149.4	-
8	149.3	-	150.5	-
9	115.7	6.97 (d, 8.5)	116.9	6.84 (d, 8.2)
10	125.9	7.16 (dd; 8.5; 2.0)	124.1	7.12 (dd; 8.2; 1.9)
2′	183.1	-	184.8	-
3′	123.2	6.53 (dd; 15.5; 3.0)	122.3	6.61 (d, 15.6)
4′	140.4	7.63 (d; 15.5)	142.1	7.59 (d, 15.8)
5′	127.9	-	128.0	-
6′	130.4	7.51 (d, 8.5)	131.5	7.51 (d, 8.7)
7′	116.0	6.89 (d, 8.5)	116.6	6.84 (d, 8.2)
8′	159.8	-	161.1	-
9′	116.0	6.89 (d; 8.5)	116.6	6.84 (d; 8.2)
10′	130.4	7.51 (d; 8.5)	131.5	7.51 (d; 8.7)
7-OCH_3	56.4	3.95 (s)	56.5	3.93 (s)
-OH		5.89 (s)		

[a] $CDCl_3$ at 600 MHz (^{1}H-NMR) and 150 MHz (^{13}C-NMR)

[#] Methanol-d_4 at 500 MHz (^{1}H-NMR) and 125 MHz (^{13}C-NMR)

3.1.3. Bisdemethoxycurcumin (BDMC)

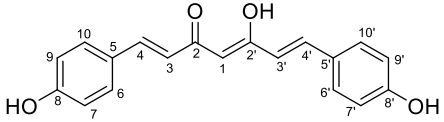

Figure 3.3. Chemical structure of BDMC

Table 3.3. ^{1}H and ^{13}C-NMR spectral data for compound BDMC

No	BDMC		[145]	
	[a]δ_C ppm	**[a]δ_H ppm (*J*; Hz)**	**#δ_C ppm**	**#δ_H ppm (*J*; Hz)**
1	100.9	5.80 (1H, s)	101.9	5.94 (2H, s)
2, 2′	183.2	-	184.8	-
3, 3′	120.8	6.53 (2H; d; 15.5)	122.0	6.60 (2H; d; 15.8)
4, 4′	140.4	7.62 (2H; d; 15.5)	141.8	7.58 (2H; d; 15.8)
5, 5′	125.9	-	128.0	-
6, 6′, 10, 10′	130.3	7.48 (4H; d, 8.5)	131.1	7.49 (4H; d, 8.6)
7, 7′, 9, 9′	115.9	6.87 (4H; d; 8.5)	116.9	6.83 (4H; d; 8.6)
8, 8′	159.8	-	161.1	-

[a] $CDCl_3$ at 500 MHz (^{1}H-NMR) and 150 MHz (^{13}C-NMR)

[#] DMSO-d_6 at 500 MHz (^{1}H-NMR) and 125 MHz (^{13}C-NMR)

3.2. Novel nematode species *S. curcumae* and its impact on turmeric chemistry and bioactivity

3.2.1. Taxonomy, molecular characteristics, and ecology

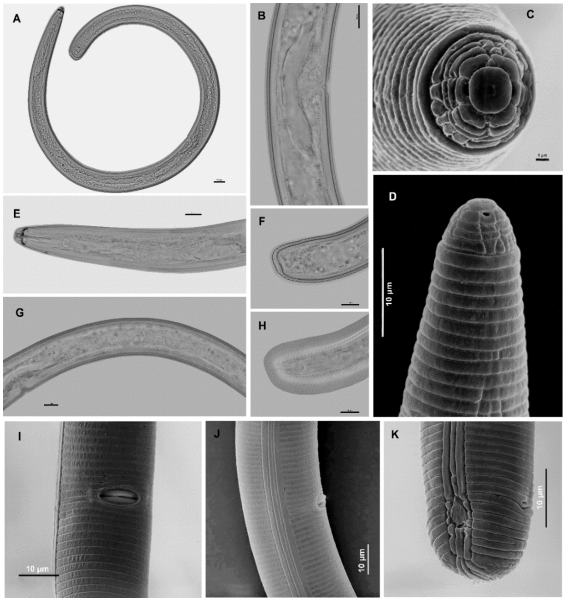

Figure 3.4. Females of *S. curcumae* from Vietnam. A: Entire body; B, I, J: Vulval region; C, D, E: Anterior region; F: Tail region; H, K: Tail region showing scutella; G: Ovary. (Scale bars: A: 200 μm; B, D-K: 10 µm; C: 1 μm).

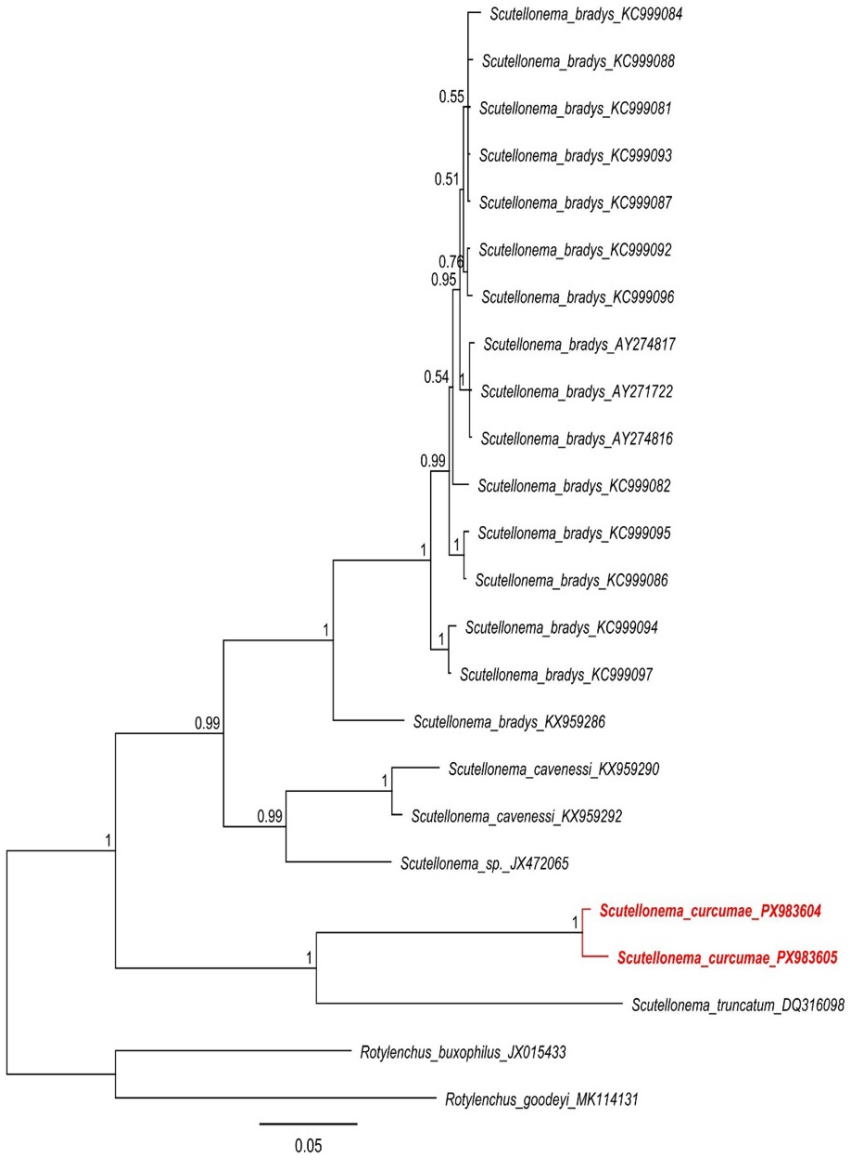

Figure 3.5. Bayesian phylogenetic tree constructed using ITS sequences of *Scutellonema* species under the GTR+G+I model. The sequence of *S. curcumae* is indicated in bold and red font.

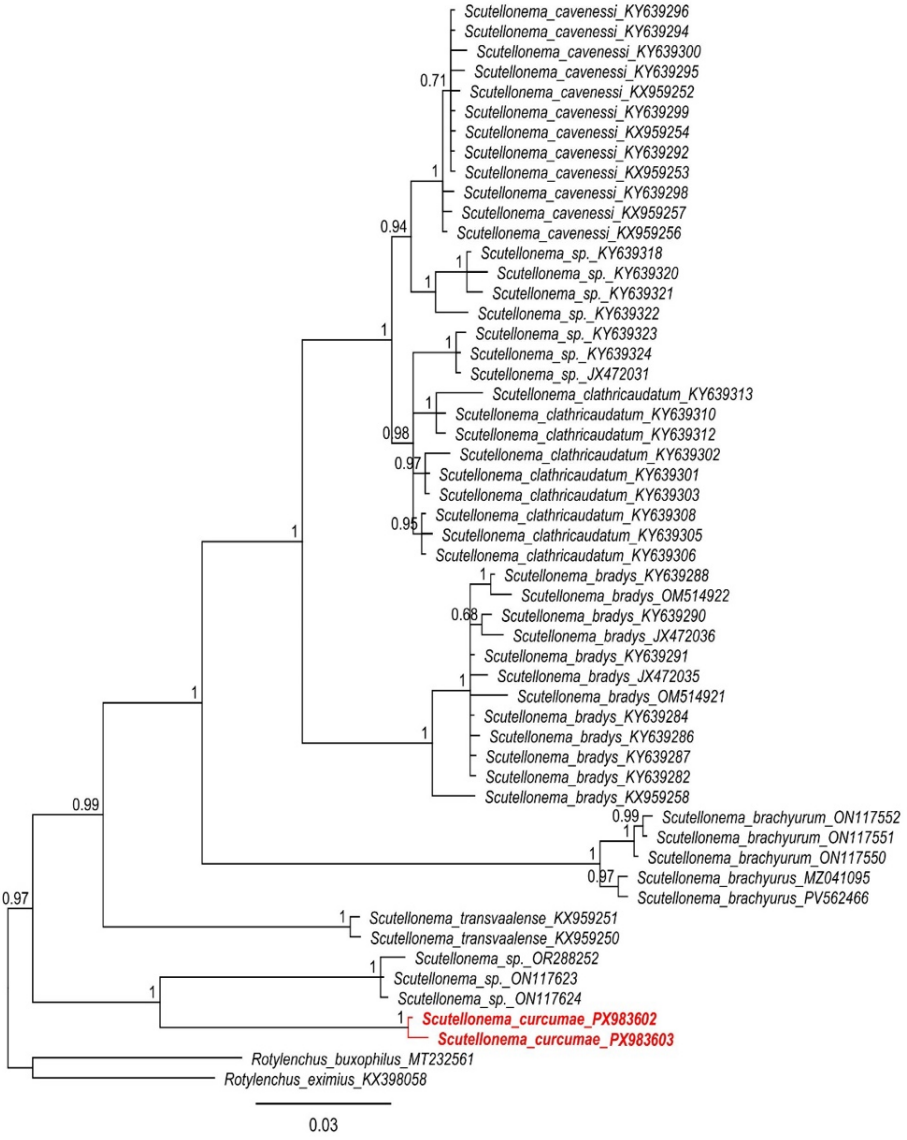

Figure 3.6. Bayesian phylogenetic tree constructed using D2-D3 sequences of *Scutellonema* species under the GTR+G+I model. The sequence of *S. curcumae* is indicated in bold and red font.

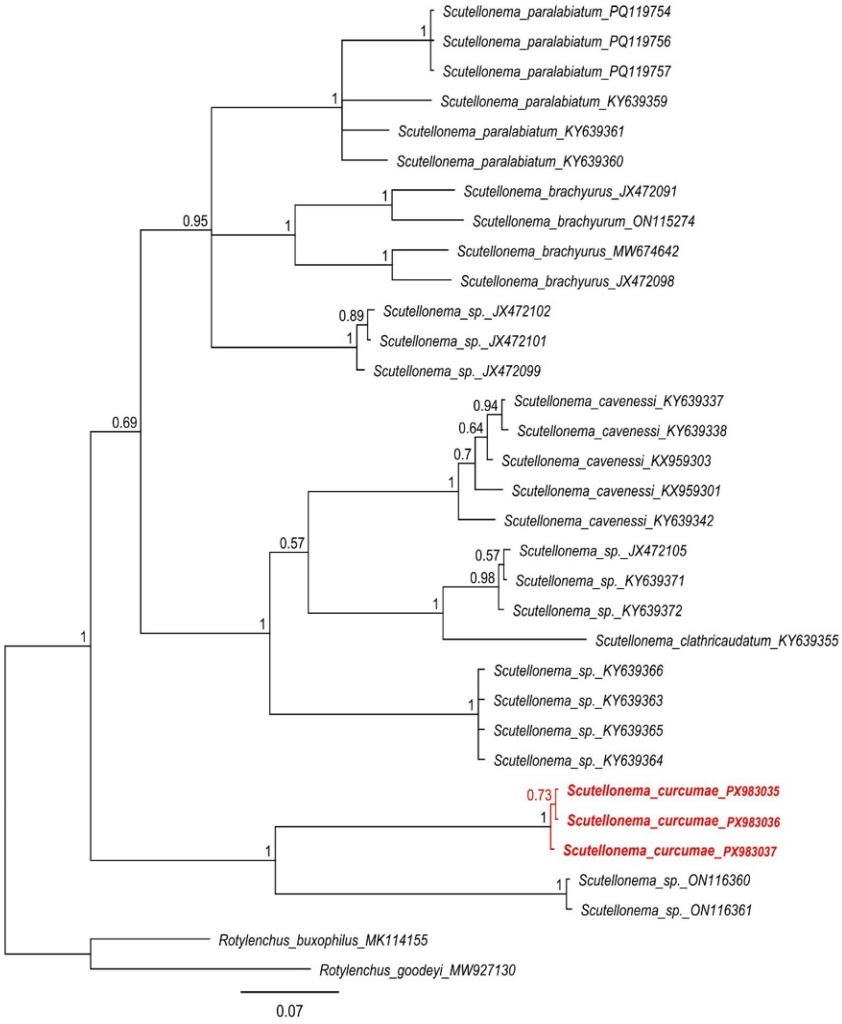

Figure 3.7. Bayesian phylogenetic tree constructed using COI sequences of *Scutellonema* species under the GTR+G+I model. The sequence of *S. curcumae* is indicated in bold and red font.

A major scientific contribution of this dissertation is the discovery and description of a novel plant-parasitic nematode species, *S. curcumae*. Morphological examination under light and scanning electron microscopy revealed characteristic features: a spiral body posture at rest, a well-

developed stylet (mean length 32 μm) enabling penetration of the hard turmeric tissues, and notably large scutella positioned symmetrically on both sides of the body at the anal level. Molecular identification using ITS, 28S, and COI gene markers confirmed the finding. Bayesian phylogenetic analysis showed that *S. curcumae* forms a distinct clade, closely related to but clearly differentiated from *S. truncatum*.

3.2.2. Changes in curcuminoid content due to nematode infestation

Table 3.4. Physicochemical properties of the soil[a] and nematode population density in the turmeric (*C. longa*) cultivation area, Kon Tum, Vietnam

Sample	pH	Moisture (%)	Total nitrogen (%)	Total nematodes (soil)[b]	Total nematodes (rhizome)[b]	*S. curcumae* (soil)[b]	*S. curcumae* (rhizome)[b]
M1	6.5	73.5	1.05	131.8	59.7	25.3	19.6
M2	6.3	73.4	0.92	58.2	17.7	11.4	7.5
M3	6.6	73.6	0.95	79.3	88.4	3.8	10.7
M4	7.1	74.1	0.98	185.3	78.4	27.9	12.5
M5	6.8	74.2	1.07	125.3	58.4	29.6	16.5
M6	6.9	74.0	1.01	141.5	66.8	22.1	12.3
M7	6.0	72.8	0.90	87.6	33.9	5.5	8.2
M8	6.2	72.9	0.91	90.2	47.9	6.3	3.1
M9	5.9	72.8	0.95	70.1	23.3	4.5	1.6
M10	5.6	70.9	0.92	36.8	11.3	2.6	0.8

[a]The soil at all sampling sites is reddish-brown basaltic soil (texture: clay loam). [b] Number of individuals per 100 g of soil/rhizome

Table 3.5. Phytochemical composition and biological activities of turmeric rhizomes in relation to nematode infestation

Sample	**Curcuminoid (%)**	**CUR (%)**	**DMC (%)**	**BDMC (%)**	**SC_{50}** (μg/ml)	**IC_{50} on Hep-G2** (μg/ml)	**IC_{50} on A549** (μg/ml)
M1	4.01 ± 0.05	3.19 ± 0.08	0.64 ± 0.04	0.16 ± 0.01	43.62 ± 3.08	44.23 ± 2.08	55.23 ± 3.34

M2	4.25 ± 0.03	3.07 ± 0.07	0.86 ± 0.02	0.32 ± 0.03	23.45 ± 2.19	43.67 ± 2.86	58.93 ± 2.99
M3	4.16 ± 0.04	3.06 ± 0.05	0.80 ± 0.03	0.31 ± 0.02	21.03 ± 2.56	45.37 ± 3.49	60.32 ± 3.05
M4	4.15 ± 0.02	3.18 ± 0.05	0.72 ± 0.02	0.23 ± 0.01	32.89 ± 3.55	38.82 ± 2.98	52.75 ± 2.45
M5	4.10 ± 0.04	3.19 ± 0.06	0.69 ± 0.04	0.21 ± 0.02	40.31 ± 3.86	37.85 ± 2.05	50.37 ± 2.97
M6	4.15 ± 0.05	3.21 ± 0.06	0.69 ± 0.01	0.23 ± 0.01	34.26 ± 3.82	38.63 ± 2.52	51.34 ± 3.14
M7	4.23 ± 0.03	3.16 ± 0.09	0.74 ± 0.02	0.31 ± 0.03	25.87 ± 2.44	39.38 ± 1.56	48.21 ± 3.82
M8	4.70 ± 0.06	3.38 ± 0.07	0.91 ± 0.03	0.41 ± 0.02	18.91 ± 1.73	35.76 ± 2.88	47.55 ± 2.43
M9	4.88 ± 0.07	3.45 ± 0.08	0.98 ± 0.04	0.46 ± 0.01	16.42 ± 1.89	29.04 ± 1.22	41.43± 3.02
M10	4.95 ± 0.02	3.45 ± 0.04	0.90 ± 0.02	0.56 ± 0.02	13.85 ± 1.31	29.35 ± 1.10	40.37 ± 3.31
Ascorbic acid		-	-	-	6.81± 1.03	-	-
Paclitaxel		-	-	-	-	47.2 ± 1.38 nM	21.3 ± 1.02 nM

Curcuminoid content variations significantly affected turmeric bioactivity. In samples with low nematode pressure, increased curcuminoid content led to markedly enhanced antioxidant activity (SC_{50} decreased from 43.62 to 13.85 μg/ml). Similarly, cytotoxic activity improved substantially, with IC_{50} values decreasing from 44.23 to 29.35 μg/ml for hepatocellular carcinoma cells (Hep-G2) and from 55.23 to 40.37 μg/ml for lung cancer cells (A549). The biological stress induced by *S. curcumae* infestation disrupted curcuminoid biosynthesis, showing a clear inverse correlation in which increasing nematode density markedly reduces the content of the curcuminoid components. This decline directly attenuated both the

antioxidant and cytotoxic activities of the raw material, underscoring the need for pest management to standardize the medicinal-material zone.

3.3. Semi-synthesis of curcumin derivatives

3.3.1. Curcumin-zerumbone semi-synthesis

Three novel derivatives were successfully synthesized: curcumin-monozerumbone (**4**) (m.p. 118-120 °C, 15% yield), curcumin-biszerumbone (**5**) (m.p. 138-140 °C, 11% yield), obtained as a yellow powder, and di-propargyl curcumin (**6**) (m.p. 128-129 °C, 21% yield). Their structures were confirmed by ^{1}H-NMR, ^{13}C-NMR and HR-MS. The spectroscopic data were fully consistent with the formation of the unsymmetrical derivative curcumin-monozerumbone (**4**) and confirmed the identity of compound (**5**) as curcumin-biszerumbone.

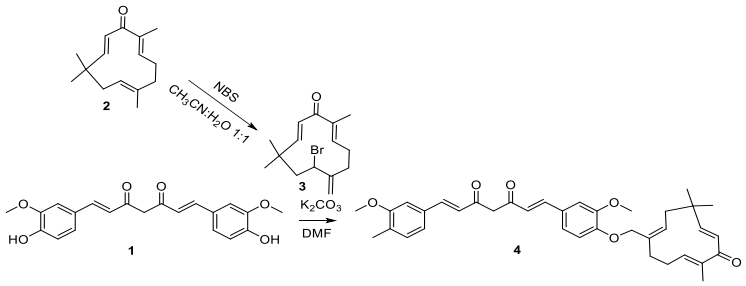

Figure 3.8. Synthesis of the curcumin-zerumbone derivatives

3.3.2. Di-propargyl curcumin semi-synthesis

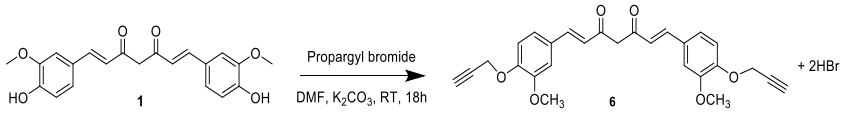

Figure 3.11. Synthesis of the di-propargyl curcumin derivative

Compound **6**, *O*,*O*′-di-propargyl curcumin, was obtained as a yellow powder (21% yield). Successful propargylation was confirmed by the methylene (–OCH_2–) signal at δH 4.89 (4H, d, J = 2.4 Hz) and the terminal alkyne (–C≡CH) at δ_H 3.61 (2H, t, J = 2.4 Hz). The curcumin scaffold retained its *trans* configuration (δ_H 7.66 and 7.07; d, J = 15.6 Hz).

3.3.3. Anti-inflammatory activity of curcumin derivatives

The anti-inflammatory activity of CUR and of the semi-synthetic derivatives (4, 5, 6) was evaluated *in vitro* from their inhibition of NO production in LPS-stimulated RAW 264.7 macrophages. Derivative (4) displayed the highest anti-inflammatory activity, with an IC_{50} of 32.15 ± 1.20 μg/ml, markedly exceeding that of CUR. Mono-substitution appears to afford a favorable spatial configuration that combines enhanced cellular permeability with multi-target inhibition arising from both structural scaffolds - the conjugated β-diketone system of the curcuminoid and the Michael-acceptor system of zerumbone - acting on the intracellular NF-κB/iNOS protein assembly. Derivative (5) likewise exhibited appreciable activity (IC_{50} = 68.20 ± 1.50 μg/ml), exceeding both CUR and derivative (6), yet remaining less potent than the mono-substituted analogue (4). The excessive steric bulk introduced by the two zerumbone moieties at either end of the molecule plausibly imposes steric hindrance, reducing conformational flexibility as the molecule approaches and binds its intracellular targets.

Table 3.7. NO production inhibitory activity and survival rate of RAW 264.7 cells treated with curcumin and its derivatives

Symbols	Compound name	IC_{50} (μg/ml)	Cell viability (%)
CUR	Curcumin	121.06 ± 2.16	82.5 ± 2.1
4	Curcumin-monozerumbone	32.15 ± 1.20	92.1 ± 1.5
5	Curcumin-biszerumbone	68.20 ± 1.50	88.2 ± 2.4
6	Di-propargyl curcumin	85.40 ± 1.85	86.4 ± 1.8
Control	Cardamonin	0.61 ± 0.24	95.0 ± 1.2

3.3.4. Cytotoxic activity of curcumin derivatives

The *in vitro* cytotoxicity of the synthetic derivatives (4), (5) and (6), together with CUR, was assessed against five human cancer cell lines: Hep-G2 (hepatocellular carcinoma), HeLa (cervical carcinoma), MCF-7 (breast carcinoma), A549 (lung carcinoma) and HGC-27 (gastric carcinoma) (Table

3.8). The semi-synthetic derivatives showed a clear improvement in activity relative to the parent curcumin. The differences in IC_{50} among the compounds provide an initial indication of how the nature of the substituent introduced at the phenolic hydroxyl position of the curcuminoid scaffold governs the resulting activity.

Table 3.8. IC_{50} values (μg/ml) of curcumin and its synthetic derivatives on 5 cancer cell lines

Symbols	IC_{50} (μg/ml)				
	Hep-G2	**HeLa**	**MCF-7**	**A549**	**HGC-27**
CUR	62.45 ± 2.15	58.15 ± 1.90	65.60 ± 2.35	72.20 ± 2.50	60.85 ± 2.05
4	25.35 ± 1.20	22.42 ± 1.15	28.05 ± 1.35	31.25 ± 1.50	26.60 ± 1.25
5	38.62 ± 1.55	35.30 ± 1.45	41.85 ± 1.70	45.45 ± 1.85	39.20 ± 1.60
6	48.15 ± 1.80	45.45 ± 1.65	52.60 ± 1.95	56.80 ± 2.10	49.35 ± 1.75
Paclitaxel	0.85 ± 0.05	0.68 ± 0.04	0.92 ± 0.05	1.15 ± 0.08	0.80 ± 0.05

3.3.5. Antimicrobial activity of curcumin derivatives

Conversion to derivative (6) broadened the activity spectrum to five strains. Activity against Gram-positive bacteria was improved (MIC reduced to 100 μg/ml), while activity against *E. coli* and two yeast strains emerged at 200 μg/ml. Derivative (4) exhibited the broadest and most potent spectrum, inhibiting 6/8 test strains: it was active against Gram-positive bacteria and the yeast *C. albicans* (MIC = 100 μg/ml), and inhibited *S. cerevisiae*, *A. niger* and *E. coli* (MIC = 200 μg/ml). By contrast, although it likewise bears the zerumbone moiety, derivative (5) showed a narrower spectrum (three strains only) and was entirely inactive against the fungi tested. Derivative (4) thus provides the clearest evidence of a successful molecular design, indicating a route towards broad-spectrum antimicrobial agents of natural origin.

Table 3.9. Results of antimicrobial activity testing of curcumin and its derivatives, sample concentrations

Sample symbol	Minimum inhibitory concentration (MIC: μg/ml)							
	Gr (-)		Gr (+)		Mold		Yeast	
	E. coli	*P. aeruginosa*	*B. subtilis*	*S. aureus*	*A. niger*	*F. oxysporum*	*S. cerevisiae*	*C. albicans*
CUR	>200	> 200	200	200	>200	>200	>200	>200
4	200	>200	100	100	200	>200	200	100
5	200	> 200	100	100	>200	>200	>200	>200
6	200	> 200	100	100	>200	>200	200	200

Values > 200 μg/ml are considered inactive at the tested concentration

3.4. *In silico* simulation results

In the LPS-stimulated RAW 264.7 cell model, BDMC exhibited superior inhibition of nitric oxide (NO) production, with an IC_{50} of 91.22 μg/ml, appreciably lower than that of CUR (121.06 μg/ml). To rationalize this observation, molecular docking showed that BDMC affords a lower binding energy (-9.73 kcal/mol) and forms more stable hydrogen-bonding interactions with the amino-acid residues lining the binding cavity of the TLR4/MD-2 receptor - a key checkpoint in the inflammatory cascade than does CUR (-9.29 kcal/mol).

Quantum-kinetic (DFT) calculations further elucidated the radical-scavenging capacity of BDMC within the lipid environment of the cell membrane. Owing to its conformationally flexible structure and the absence of sterically hindering methoxy groups, BDMC exhibits a rate constant for HOO• radical scavenging substantially higher than that of curcumin. ADMET predictions likewise indicated that BDMC possesses favorable pharmacokinetic characteristics, low toxicity and a high absorption potential.

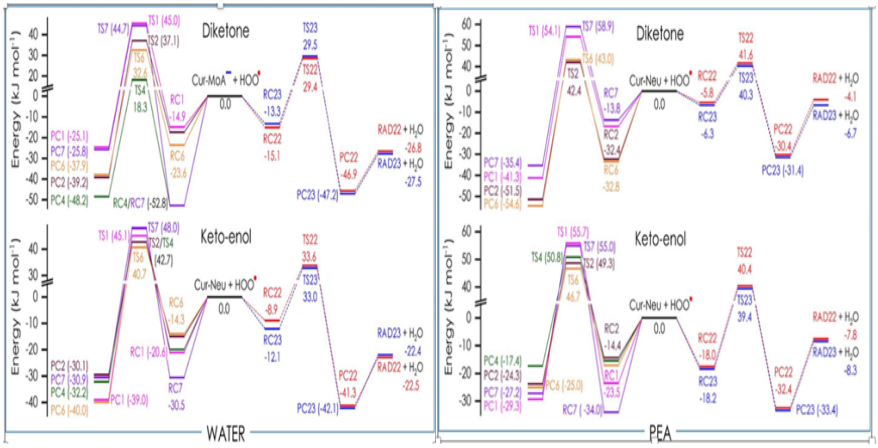

Figure 3.13. Relative enthalpy profile corrected for Zero Point Energy (ZPE) at 0 K for abstraction and addition reactions initiated by the HOO• radical for CUR in water and PEA.

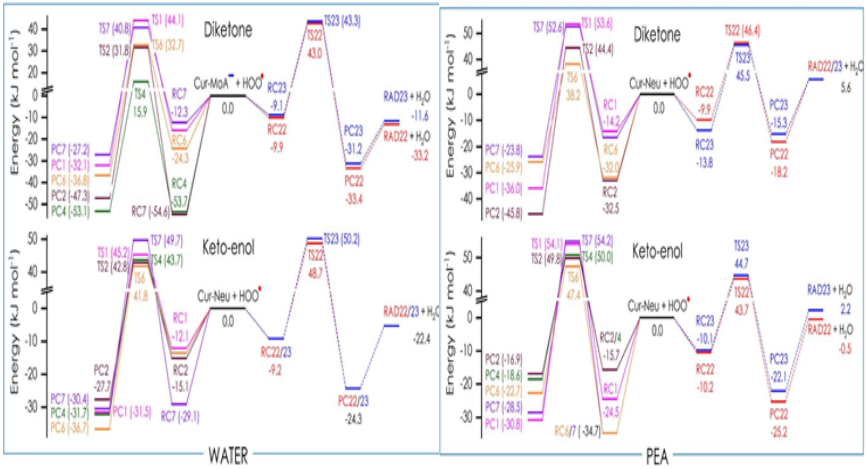

Figure 3.14. Relative enthalpy profile corrected for Zero Point Energy (ZPE) at 0 K for abstraction and addition reactions initiated by the HOO• radical for BDMC in water and PEA.

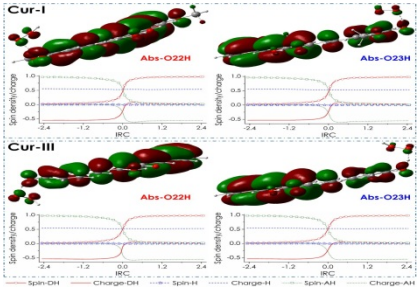

Figure 3.15. Evolution of the spin density and the NPA charges of the donor centre (DH), the transferred hydrogen (H) and the acceptor centre (AH) along the intrinsic reaction coordinate (IRC), together with the SOMO orbital at the transition state (TS), for the predominant PCET reactions in the aqueous phase.

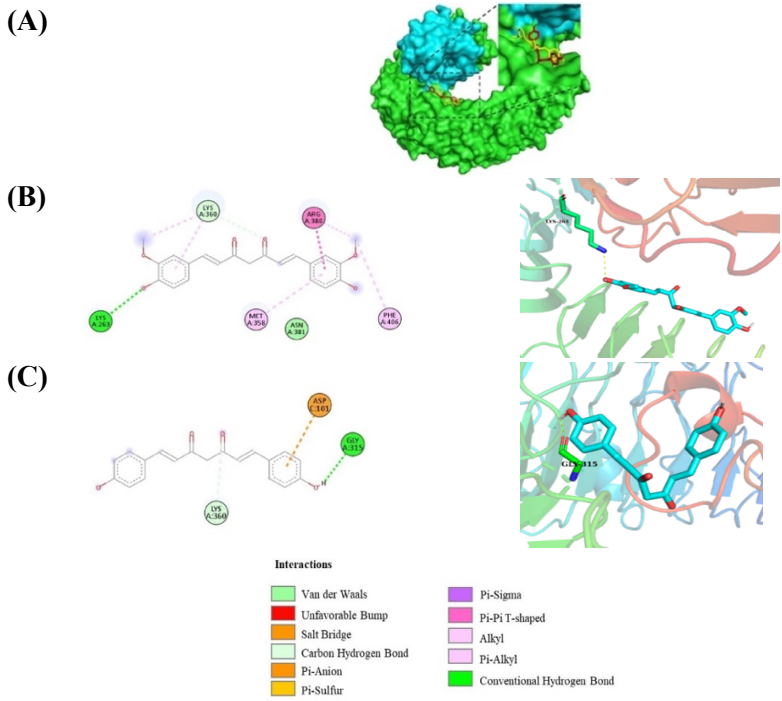

Figure 3.16. Interactions of CUR and BDMC within the TLR4/MD-2 complex obtained using AutoDock4. (A) The investigated compounds bind to a region on TLR4, adjacent to its interface with MD-2: CUR in red, BDMC in yellow; (B) Docking pose of CUR; (C) Docking pose of BDMC.

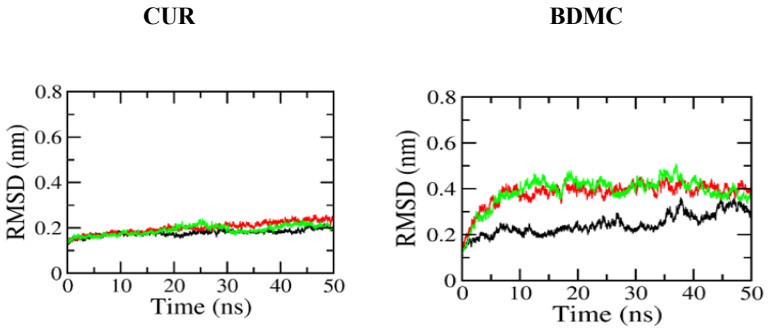

Figure 3.17. All-atom RMSD of TLR4/MD-2 with CUR (A) and BDMC (B) over three independent 50 ns MD simulation runs.

CUR and BDMC possess physicochemical properties well suited to oral absorption and comply fully with Lipinski's rule of five; compound (4) violates a single criterion yet still conforms to the rule overall. The consistency among the pharmacokinetic models, the MD simulation results and the affinity scores from AutoDock4 indicates that these natural derivatives are promising TLR4/MD-2 inhibitors with viable pharmacological properties. Their assignment to toxicity classes 4 and 5, together with favorable predicted LD50 values, indicates a wide safety window and supports the pursuit of subsequent drug-development studies.

Table 3.16. ADMET indices and toxicity predictions of potential compounds

Compound	**MW**	**HBD**	**HBA**	**LogP**	**MR (cm^3/mol)**	**TPSA (Å²)[a]**	**LD_{50} (mg/kg)**	**Predicted toxicity[b]**	**HIA (%)**
CUR	368	2	6	3.72	102.80	93.06	2000	4	93.30
BDMC	308	2	4	3.24	89.82	74.60	2560	5	94.20
4	486	1	5	6.51	165.56	85.00	2300	5	92.80

[a]Topological polar surface area; [b]Predicted toxicity classification: 1 → 6 (highly toxic to non-toxic).

CUR and BDMC both exhibited pronounced inhibitory efficacy against NO production in macrophages and against the proliferation of cancer cell lines. Among them, BDMC emerges as a promising candidate, combining potent anti-inflammatory activity through iNOS inhibition with selective effects on drug-resistant cancer cell lines. The *in silico* studies confirmed and rationalized the structural advantage of BDMC: the absence of conformationally flexible methoxy groups allows BDMC to optimize its spatial interactions and hydrogen-bonding network, thereby forming thermodynamically more stable complexes with the key protein target TLR4/MD-2.

ADMET analysis indicated that the curcuminoids, and BDMC in particular, possess favorable pharmacokinetic profiles and a high margin of safety (toxicity classes 4 and 5), reinforcing the case for their development as potential therapeutic agents. These findings would benefit from *in vivo* validation in animal models of inflammation or cancer to confirm the therapeutic efficacy and systemic safety of BDMC, and from molecular-biological techniques (Western blot, qPCR and ELISA) to elucidate the regulation of the computationally predicted NF-κB, STAT3 and iNOS signaling pathways.

The *in silico* approach successfully elucidated the mechanisms of action at the molecular level, in close agreement with the *in vitro* results. Specifically, quantum-chemical (DFT) calculations clarified the solvent dependence of the antioxidant mechanism: the aqueous environment favours single-electron transfer (SET) from anionic species, whereas the lipid environment favours proton-coupled electron transfer (PCET). Regarding anti-inflammatory activity, MD simulations demonstrated that BDMC and the methoxy-deficient derivatives form more stable electrostatic and hydrophobic binding interactions with the TLR4/MD-2 target protein complex than does CUR.

CONCLUSIONS

The principal conclusions drawn from this dissertation are as follows:

1. Three pure curcuminoids: CUR, DMC and BDMC were successfully extracted, isolated and structurally characterized from the rhizomes of turmeric (*C. longa*) collected in Vietnam.

2. The novel parasitic nematode species *Scutellonema curcumae* on turmeric roots was discovered and molecularly identified for the first time. An inverse correlation was established: an increasing density of nematode infestation reduces the curcuminoid content, thereby lowering the antioxidant and cytotoxic activities of the medicinal material.

3. Three novel curcumin derivatives were successfully semi-synthesized and structurally characterized through modification at the phenolic hydroxyl group, comprising the di-propargyl-substituted derivative (*O,O′*-di-propargyl curcumin) and the zerumbone-hybridized derivatives (curcumin-monozerumbone and curcumin-biszerumbone).

4. With respect to *in vitro* biological activity, a structure–activity relationship was demonstrated: (i) BDMC exhibited anti-inflammatory activity superior to that of CUR (NO-inhibition IC_{50} of 91.22 μg/ml versus 121.06 μg/ml); (ii) the mono-substituted hybrid curcumin-monozerumbone showed the highest potency, markedly improving anti-inflammatory activity, exhibiting stronger inhibition than CUR against Hep-G2 hepatocellular carcinoma cells, and broadening the antimicrobial spectrum.

5. With respect to *in silico* evaluation, the molecular basis of the biological activities was successfully elucidated: (i) DFT calculations confirmed that single-electron transfer (SET) and proton-coupled electron transfer (PCET) play the dominant roles in radical-scavenging activity; (ii) molecular docking and molecular dynamics (MD) simulations demonstrated that the methoxy-free structure of BDMC optimizes spatial interactions, forming the most stable electrostatic and hydrophobic complex with the TLR4/MD-2 target protein (binding energy -9.73 kcal/mol), which accounts for the pronounced anti-inflammatory efficacy of BDMC observed experimentally.

RECOMMENDATIONS

Based on these findings, three directions for further research are proposed:

1. Further *in silico* studies (molecular docking and MD simulation) should be pursued on the novel hybrid derivatives (curcumin-monozerumbone, curcumin-biszerumbone) against a range of protein targets, to elucidate their molecular basis more fully and to guide the design of optimized drug-like structures.

2. Artificial-inoculation experiments (following Koch's postulates) should be conducted under greenhouse conditions to investigate in depth the pathogenic mechanism of the novel nematode species *S. curcumae* on turmeric, together with *in vivo* assays to evaluate the biological activities of the isolated compounds.

3. The ecological findings of this study should be applied as a scientific basis for further research in Agronomy and Plant Protection - developing biological agents for nematode control or adjusting cultivation practices such as soil-pH management with a view to securing and enhancing the quality of turmeric as a medicinal material in Vietnam.